STUDY OF MAGNESIUM OXYSULFATE (MOS) MATRICES REINFORCED WITH FIBERGLASS AND LIMESTONE FILLER FOR APPLICATIONS IN CIVIL CONSTRUCTION

Kalita C. Araujo[1] Antonio P. Peruzzi[1] Carlos E. M. Gomes[2]
[1]Department of Civil Engineering, Universidade Federal de Uberlandia, Uberlandia, MG, 38.400-902, Brazil
kalita.araujo@ufu.br, aperuzzi@ufu.br
[2]Department of Civil Engineering and Architecture, Universidade de Campinas, Campinas, SP, 13.083-862, Brazil
cemgomes@unicamp.br

ABSTRACT

This study evaluated Magnesium Oxysulfate (MOS)-based matrices reinforced with AR glass fibers and limestone addition for applications in civil construction. Examined how the use of fiberglass and limestone affected the mechanical and physical characteristics of MOS and the adhesion between matrix-fiberglass in this composite aiming for the Dimensional Stabilization of the composite, reducing its propensity to cracking, and reducing the final cost of the composite. Mechanical and Physical assays were performed and observations by SEM on samples cured at room temperature. The results showed that the addition of limestone content, above a certain quantity, improves the behavior of the MOS increasing its Flexural Strength, was beneficial for the Dimensional Stabilization of the composite, reducing its propensity to cracking, but high levels of limestone compromised the mechanical properties of the composite, due to the reduction of the Molar Ratio and the inert behavior of the limestone. Substitution levels between 10% and 20%, the pores formed acted to relieve internal tensions generated by the expansion of MgO, resulting in an improvement in Flexural Strength. The addition of fiberglass, proved to be effective in controlling shrinkage, preventing the formation of cracks and increasing tensile and Flexural Strength, like the behavior observed in Portland cements.

KEYWORDS: *Magnesium Cement, Magnesium Oxide Composite, MOS, Powdered Limestone*

I. INTRODUCTION

Research on Magnesium Oxide (MgO) cements as a sustainable option for civil building materials has been driven by lower energy consumption and CO_2 emissions during manufacture [1, 2, 3, 4]. Various studies indicate that MgO-based concrete can achieve a Compressive and Tensile Strength superior to that of conventional concrete, and its performance increasing how the amount of MgO increase, vary the curing conditions, and the age of the material [5].

The addiction of mineral mixtures causes the improvement of the properties of MgO composites, resulting in greater Mechanical Resistance, mainly due to increased density. Recent studies indicate that partial replacement of MgO with carbonates, such as $CaCO_3$ and $MgCO_3$, improve Flexural Strength of the composites, although in some cases this affect the Compressive Strength too [6, 7, 8, 9, 10, 11, 12]. The more neutral pH of MOS, if compared to Portland cement, makes this composite more suitable for used with fibres susceptible to alkaline attack, such as fiberglass [13, 14]

This work aims to investigate MOS composite, replacing part of the MgO by powdered limestone, and addiction of fiberglass alkali-resistant (AR) to improve its Flexural properties. The partial replacement of MgO by Calcium Carbonate ($CaCO_3$), in a range of 10% to 40%, was made to provide Volumetric Stability, beyond reduce Shrinkage, and to reduce the final cost of the composite. Limestone is an

abundant and easily accessible material, and for this reason, he was chosen. Beyond it is a material widely used in cement composites such as fiber cements whose technology of application is widely mastered. AR fiberglass was chosen to reinforce the composite, aiming to provide lightness, mechanical and chemical resistance, as well as an attractive cost-benefit, and the fiberglass incorporation varied from 1% to 3%.

The remainder of the text is organized as follows: Section II presents the materials and methodology employed; results and discussion are presented in Section III and the main conclusions drawn from the study are presented in Section IV.

II. METHODOLOGY

2.1. Materials

The composite studied was produced using Magnesium Oxide (MgO), Magnesium Sulfate Heptahydrate ($MgSO_4 \cdot 7H_2O$, also known as Epsom salt), water, limestone ($CaCO_3$) and fiberglass Alkali Resistant (AR). MgO was produced from the calcination of natural $MgCO_3$ in a rotary kiln at a temperature below 1,200°C, and its purity content was approximately 90%. MgO particle size showed D_{90} of 62.5 µm and D_{50} of 23.5 µm. X-ray diffraction of MgO was used, and Table 1 shows its distribution. Granulometric distribution is shown in Figure 1.

Table 1. MgO chemistry composition.

Mass Percentage (%)					
MgO	SiO_2	Al_2O_3	Fe_2O_3	CaO	MnO
90.0	4.0	0.3	3.5	2.0	0.2

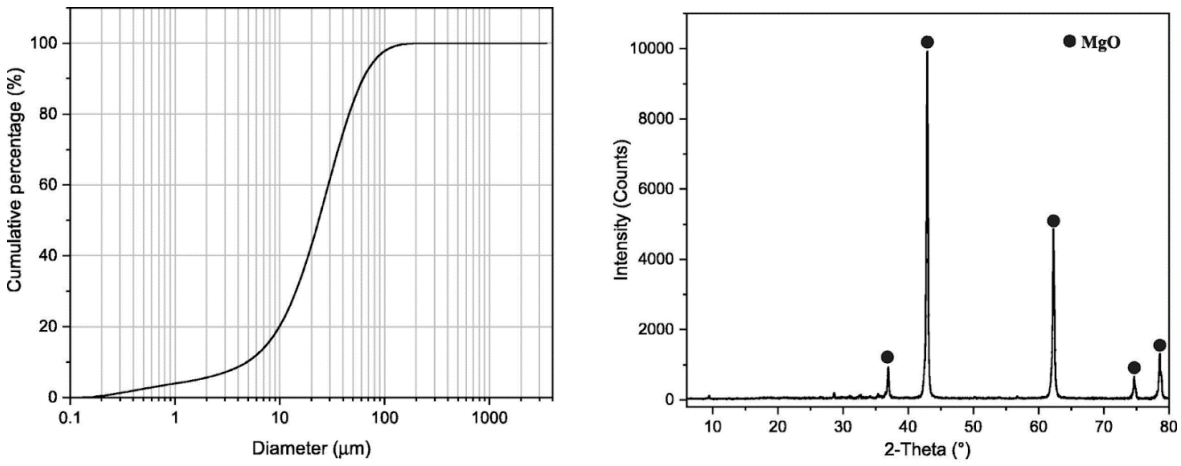

(a) (b)

Figure 1. a) grain size distribution curve **b)** X-ray diffraction

The liquid phase was prepared diluting Epsom salt - with a purity of approximately 97% - in water, resulting a solubility of 500 g/L. Calcium Carbonate used was powdered limestone, standard type, used in the fiber cement industry, with D_{90} of 100.05 µm and D_{50} of 24.3 µm. Figure 2 shows the X Ray Diffraction of the limestone powder.

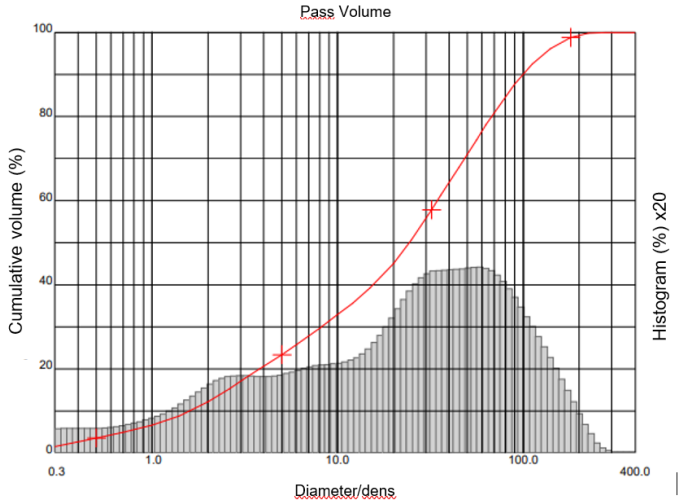

Figure 2. X-ray diffraction of the limestone powder (Source: ULTRAFINE TECH, 2018)

AR fiberglass used was Cem-FIL brand type "HP 12 anti-crack" (Figure 3) that have a length of 12 mm, length/diameter ratio of 58, an equivalent diameter of 0.2 mm. Its Modulus of Elasticity (E) is 72 GPa, Tensile Strength 1,000 MPa, and Density 2.68 g/cm³.

Figure 3. Chopped AR fiber glass used

2.2. Types of samples

First, were developed and evaluated different formulations of the MOS, defining a concentration of 162 g/L of $MgSO_4$ from the dilution of 40% of Epsom Salt in water to enable the chemical reactions of the composite. Saltwater/solids (SA/P) ratio of 0.65 was determined and $MgSO_4/H_2O$ molar ratio of 2.38 was fixed, and from that onward only the $MgO/MgSO_4$ molar ratio (referred to as "M") was varied. Then, were created five compositions, varying the substitution content of MgO by limestone, with four proportions with $CaCO_3$ (10%, 20%, 30%, 40%) added to the reference sample without limestone (M_0, 0%). These proportions were chosen because some studies indicated that substitution rates of up to 40% could improve flexural properties, while higher quantities tend to compromise Compressive Strength. Thus, the values of Molar Ratio (M) were adjusted for each composition: M_0 (11.39), M_{10} (10.25), M_{20} (9.11), M_{30} (7.97), and M_{40} (6.63), with all formulations maintaining a M above 5, which is considered ideal for the material's performance. Next, fiberglass - MOS interaction were investigated, focusing on the impact that the fibers represent on the mechanical properties, especially Flexural Strength, mainly regarding the adhesion fiber-matrix. The two composites with the best mechanical performance in the flexure of the 1st phase of the research (only limestone filler added, without fiber) were selected for the addition of AR fiberglass. The fiberglass (chopped fiber) was chosen due to their advantages such as high Modulus of Elasticity, Lightness and Tensile Strength, in addition to being attractive cost-effective.

An exploratory study was carried out with the composite M_{10} (with lower limestone content) to determine the ideal quantity of fibers, varying the additions of fiberglass from 0.5% to 3% (in volume), to ensure good molding and mechanical reinforcement without compromising consistency.

2.3. Preparing of Samples

Concentration of $MgSO_4$ was obtained by diluting 40% Epsom salt in water, establishing the Saltwater/solid (SW/s) ratio at 0.65, and fixing a molar ratio of $MgSO_4/H_2O$ at 2.38; thus, only the molar ratio of $MgO/MgSO_4$ was varied. Table 2 shows the composition of the samples studied. Samples M_{10} and M_{20} were chosen and contents of 1%, 2% and 3% of fiberglass were added, giving rise to samples M_{10} 1%, M_{10} 2%, M_{10} 3% and M_{20} 1%, M_{20} 2%, M_{20} 30%.

Table 2. Composition of samples of composites without fiber

Sample	MgO (%)	$CaCO_3$ (%)	$MgSO_4$ (g/l) concentration	SW/s ratio	Molar ratio MgO/$MgSO_4$	Molar ratio $H_2O/MgSO_4$
M_0	100	0	162	0,65	11,39	2,38
M_{10}	90	10	162	0,65	10,25	2,38
M_{20}	80	20	162	0,65	9,11	2,38
M_{30}	70	30	162	0,65	7,97	2,38
M_{40}	60	40	162	0,65	6,63	2,38

The sample of each mixture was prepared was as follows:

1st) Dilute of the Epson salt in water until to form a 162 g/L solution, using a magnetic stirrer for 1 minute at fast speed, at room temperature. Then the solution was reserved;

2nd) predetermined amounts of MgO were mixed with the limestone, and homogenized forming a dry mixture (for samples M_{10}, M_{20}, M_{30} and M_{40});

3td) To the dry mixture was added saltwater, and with an electric mixer, it was homogenized for 5 minutes (see Figure 4a);

4th) Each type of sample was placed in prismatic molds of 40mm × 40mm × 160mm (see Figure 4b).

Figure 4c shows the samples already out of the molds and identified. For the samples with fibres added, right after the total dilution of the mixture (3rd step), the contents of fiberglass were added and mixed manually for approximately 5 minutes, until a perfect homogenization of the fibres in the composite was obtained.

Figure 4. Sequence of the preparation of samples

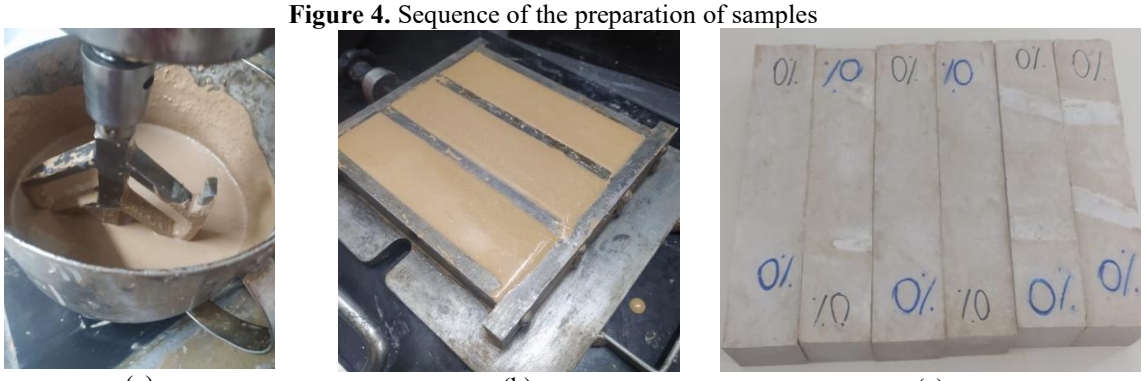

(a) (b) (c)

2.4. Tests performed

Consistency in the fresh state of each type of sample was made using Standard [15] (see Figure 5a). Density was determined according to the Standard [16]. Specimens of Le Chatelier Apparatus for determination of Expandability were tested by Standard [17] (see Figure 5b).

(a) (b)

Figure 5. a) Consistency in the fresh state test made by ABNT NBR 13276:2016; **b)** Determination of expandability (Le Chatelier Apparatus) by BS EN 196-3:2016

Flexural Strength was determined according to Standard [18] and the tests were performed in a BIOPDI universal testing machine with an approximate speed of 50 N/s (see Figure 6a). Compressive Strength was determined according to Standard [19]. The testing machine used was the same as the flexure test, with an approximate speed of 500 N/s (see Figure 6b).

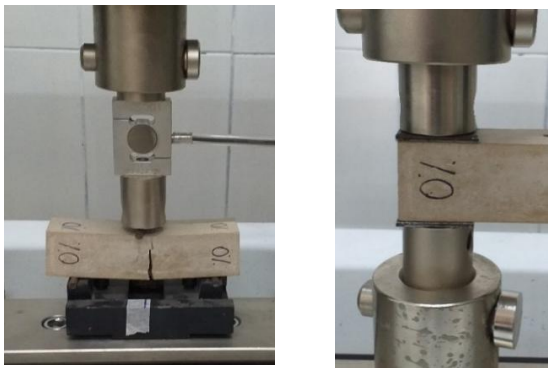

(a) (b)

Figure 6. a) Flexural Strength test made by ASTM C348–02 **b)** Compressive Strength by ASTM C349-02

2.5. Microstructure analysis

MEV of the samples with fractured surfaces was analyzed by Scanning Electron Microscopy (SEM). The equipment used was the Tescan VEGA 3 LMU of the Chemistry Institute of University Federal of Uberlandia.

2.6. Statistical analysis of results

Statistical purification of the results was made using Chauvenet criterium.

III. RESULTS AND DISCUSSION

3.1. Consistence

Figure 7a shows the results obtained in the Consistency tests of samples M_0, M_{10}, M_{20}, M_{30} and M_{40} in samples without fibres. In it we see that, as the molar relationship decreased with the increase in the replacement of MgO by limestone, the fluidity of the composite increased. The reduction of the

MgO/$MgSO_4$ molar ratio increase the limestone content resulting a greater amount of water available in the paste. Limestone used has a larger particle size than MgO, which may have affected the system, contributing to greater fluidity. In addition, the high amount of water in the paste - resulting from the AS/P=0.65 ratio and the water present in the $MgSO_4 \cdot 7H_2O$ - may also have influenced the increase in fluidity. As expected, when fiberglass was added, the consistency decrease (see Figure 7b).

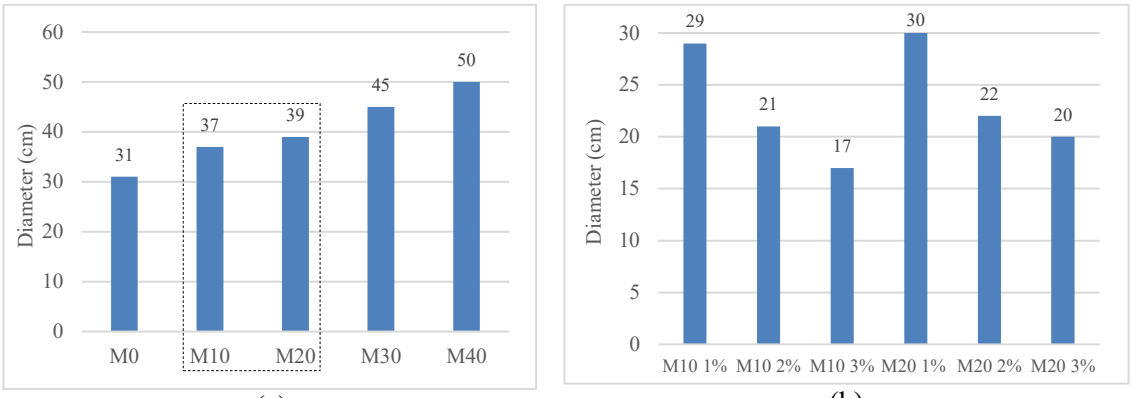

(a) (b)

Figure 7. a) Composites' Consistence without fibre **b)** Composites' Consistence fibre added

3.2. Density

Figure 8 shows the Density of the samples tested without fibres and with fibres added.

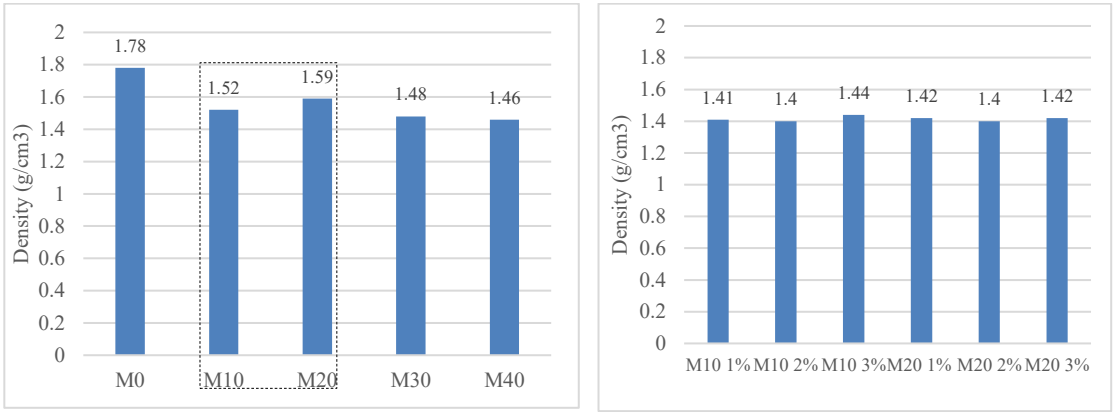

(a) **(b)**

Figure 8. a) Density of samples without fibre **b)** Density of samples with fibre added

M_0, with higher MgO content, showed higher density (1.78g/m^3), followed by M_{10} (1.52g/cm^3), M_{20} (1.59g/cm^3), and M_{30} (1.48g/cm^3). M_{40}, with higher limestone content, possibly there was more porous, and this factor resulted in lower density (1.46g/m^3) in the sample (Figure 8a). The addition of fiberglass resulted in a decrease in Density and an increase in the Porosity of the all samples (see Figure 8b): M_{10} with 3% fiber had a Density of 1.44 g/cm^3 representing a reduction of 5.3%; M_{20} with 3% fiber was 1.42 g/cm^3 with a reduction of 10.7%. As expected, the addition of fibers increases Porosity.

3.3. Expandability from Le Chatelier test

The Dimensional Variation was measured at three different moments: 1st) before the beginning of the set, 2nd) after the end of the setting and 3rd) next seventh day of curing and aimed to analyse the "retraction" (-) and "expansion" (+) of the samples (Table 5). A continuous shrinkage behaviour was observed during the curing process at room temperature for the M_0 sample (Reference), and the retraction was more pronounced before the "onset of grip", stabilizing after that point.

Table 5. Dimensional variation of samples without fiber

Sample	Begginin of setting	End of setting	7 days
M_0	-2.30	-2.25	-2.25
M_{10}	-1.15	-0.50	+0.40
M_{20}	+0.40	-0.60	+0.85
M_{30}	-0.60	+0.50	+1.50
M_{40}	-1.30	-0.80	+0.70

Obs.: (-) Retraction (+) Expansion

The test was carried out for the samples M_{10} and M_{20} with the highest percentage of fibres used in this research (3%), with the intention of to verify and confirm the effectiveness of the fiberglass in controlling the dimensional variation (Table 6). The test was also performed in the M_0 sample, since this sample presented the greatest dimensional variation in the test performed in 1st phase of experiments (without fiber).

Table 6. Dimensional variation of samples with fiber added

Sample	Begginin of setting	End of setting	7 days
M_0 3%	-0.45	+0.85	+0.80
M_{10} 3%	-1.05	+0.83	+0.80
M_{10} 3%	-0.70	+0.58	+0.35

Obs.: (-) Retraction (+) Expansion

3.4. Flexural Strength

Figure 9 shows de results of Flexural Strength obtained by tests in a) samples that did not receive the addition of fiberglass, and b) samples with fiberglass added.

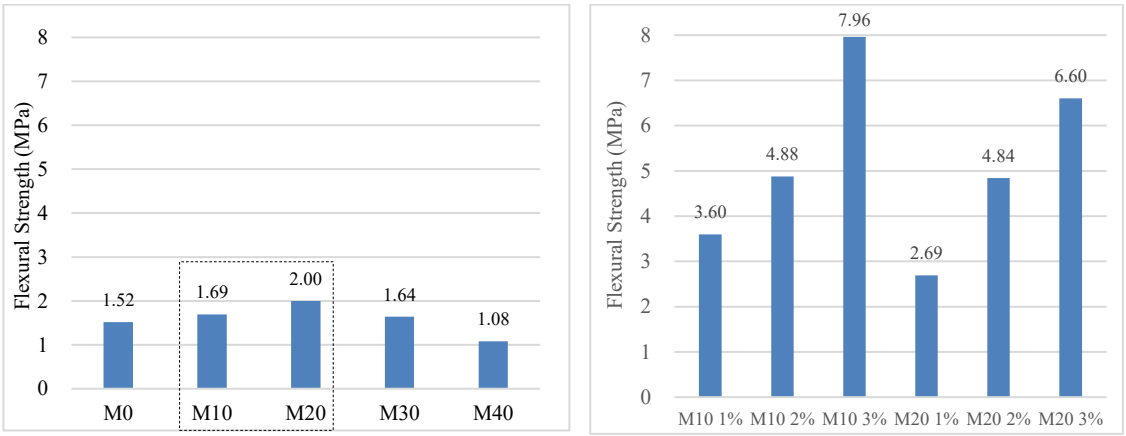

(a) (b)

Figure 9. a) Flexural Strength samples without fiber **b)** Flexural Strength samples with fiber added

Samples with up to 20% MgO substitution for limestone (M_{20}) (see Fig. 9a), showed a significant improvement in Flexural Strength with 32% increase in Flexural Resistance compared to the M_0 (Reference). However, from 30% replacement (M_{30}), Flexural Strength began to decrease as the M_{40} sample showing a 29% reduction in Flexural Strength compared to M0. As expected, the Flexural Strength was increased with the addition of the fiberglass (see Fig. 9b), especially M_{10} 3% sample (with 3% fiberglass added), showed 79% increase in strength in relation to M_{10}. M_{20} 3% also had a considerable increase in Flexural Strength (70%), compared to the M_{20} sample without fiberglass.

3.5. Compressive Strength

Figure 10 shows the results of Compressive Strength obtained a) samples that did not receive the addition of fiberglass, and b) samples with fiberglass added.

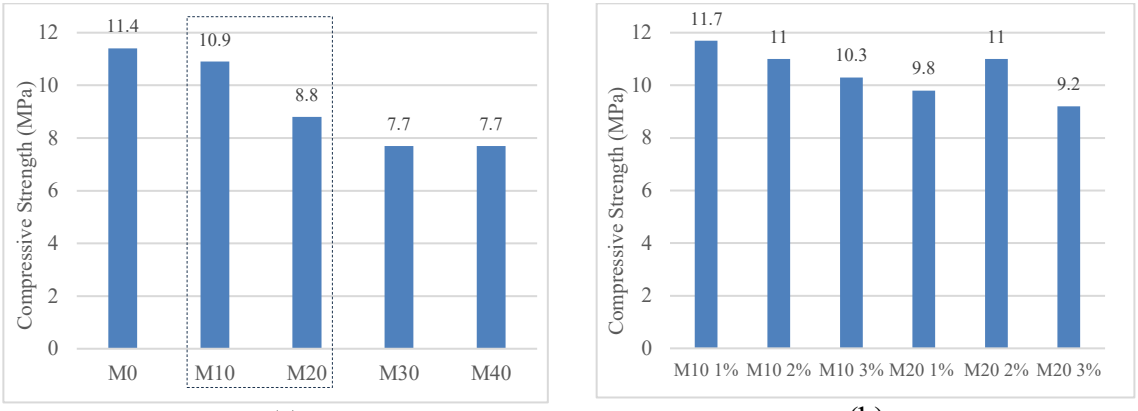

Figure 10. a) Compressive Strength samples without fibre b) Compressive Strength samples with fibre added

When limestone was added, Compressive Strength decrease, especially in the samples with 40% limestone (M_{40}), which showed a 33% drop compared to the "Reference" sample M_0 (see Fig. 10a). This effect, possibly, can be explained by the phenomenon of dilution, in which the substitution of MgO by limestone - an inert material - reduces the amount of hydration products formed, increasing the fragility of the material structure. The hydration phases of MOS - such as Phases 3 and 5 - form at a lower intensity or do not form at all in samples with higher limestone content, which contributes to the minor Compressive Strength. In this study, the replacement of MgO by limestone reduced this Molar Ratio which, probably, contributed to the decrease in the strength of the material. Analysing the influence of the addition of fiberglass in the Compressive Strength, comparing M_{10} (see Fig. 10a) and Figure 10b the addition of fibres did not significantly influence the result, regarding M_{20} samples (M_{20} 1%, M_{20} 2%, and M_{20} 3%) fiberglass addition exerted a greater influence leading to the increase of resistance.

3.6 Microstructure

Microstructure Analysis made in samples of composites without fibres aimed observe the type of MOS cement hydration phases formed, mainly 5-1-7 Phase ($5Mg(OH)_2 \cdot MgSO_4 \cdot 7H_2O$), called 5-Phase, because it is mechanically resistant, stable in aqueous medium and hardly decomposes at pH below 12.

Sample without the addition of lime (M_0) is shown in Figure 11a, and the microstructure is mainly composed of crystalline particles of $Mg(OH)_2$, a typical feature of MgO compounds. **Leaf rosettes** and **hexagonal blocks**, which are characteristic of the formation of $Mg(OH)_2$, was observed. In addition, **hexagonal plates** can be observed, indicating the presence of hydration 3-Phase, which is confirmed by EDS analysis, in which, along with Magnesium and Oxygen, Sulfur is also identified, resulting in a sulfated compound that characterizes 3-Phase.

Figure 11b shows M_{10} microstructure, through which is possible to verify the formation of hydrated $Mg(OH)_2$, besides the presence of more circular and spherical pores. These spherical pores are distinct from capillary voids, since, despite reducing Density, they do not allow water to pass through, which does not negatively affect Mechanical Resistance. In addition, the replacement of MgO by 10% limestone results in an increase in Flexural Strength, and the spherical pores may have relieved the internal tension generated by the expansion of MgO hydration, which is one of the factors that contribute to the improvement of the observed dimensional variation.

Figure 11c shows the morphology of M_{20} in which it is possible to perceive the formation of **hexagonal blocks**, probably due to the presence of 3-Phase, indicated by the EDS, which reveals a high concentration of Sulfur. In addition to the **rosettes** that indicate the formation of $Mg(OH)_2$. EDS also

shows a high concentration of Calcium, derived from the greater presence of limestone in the sample. The combination of these elements results in a denser structure, which corroborates the higher Density results obtained for M_{20}.

M_{30} microstructure (see Fig. 11d) exhibits the characteristic morphology of Magnesium Hydroxide, but with a more porous appearance and a less dense structure. It can be assumed that this morphology may be the factor responsible for the decrease in resistance observed in samples with higher limestone content.

M_{40} morphology is shown in Figure 11e, and the formation of Magnesium Hydroxide is observed, with limestone particles due to the higher limestone content in the sample. The morphology reveals a greater presence of inert materials and tiny hydration of MgO, reflecting negatively on Mechanical Resistance. The formation of **needle-shaped** structures was also observed, associated with the high concentration of Sulfur shown by EDS. This may indicate the formation of hydration 5-Phase, which, although present, does not occur in sufficient quantity to improve the mechanical performance of M_{40}. 5-Phase needles tend to form in voids and are unstable at low temperatures, which may have been the reason for their limited formation, as the cure, in this case, was performed at room temperature.

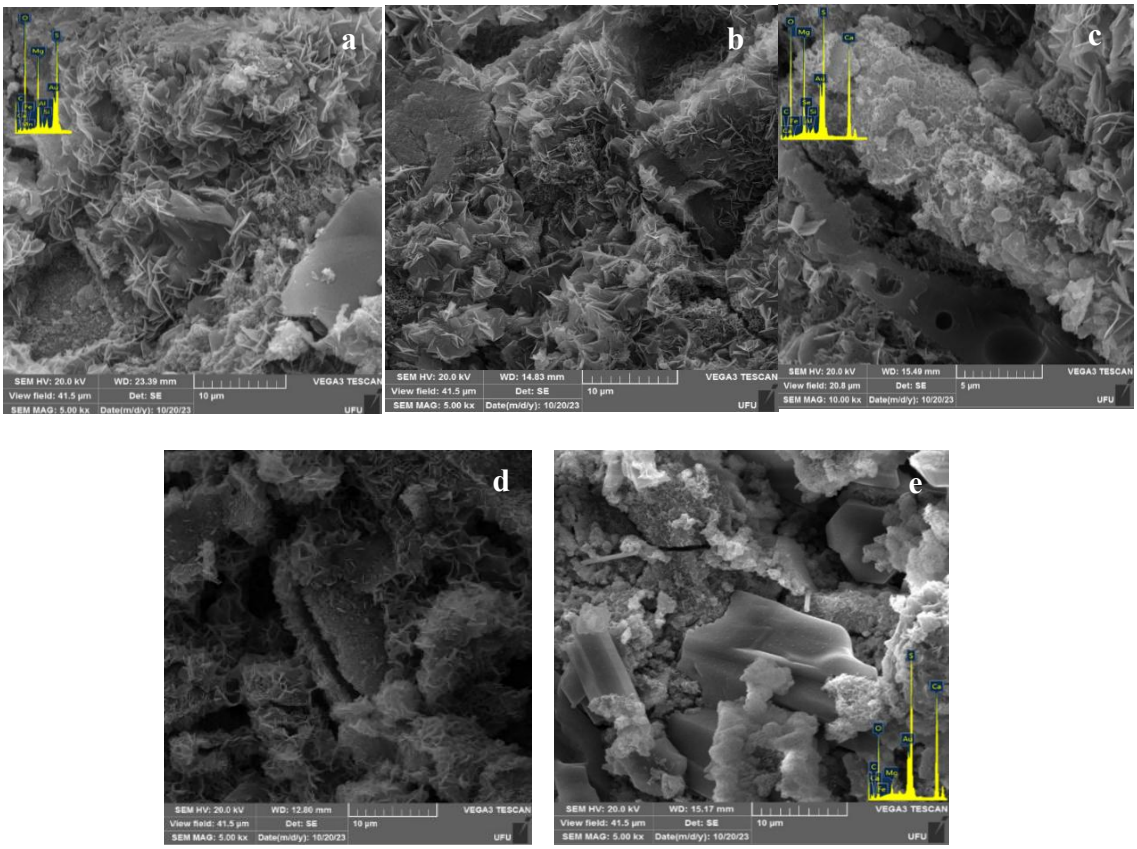

Figure 11. SEM imagens from MOS composites without fiberglass. **a)** M_0 (0% limestone added – Reference) **b)** M10 (10% limestone added) **c)** M20 (20% limestone added) **d)** M30 (30% limestone added) **e)** M40 (40% limestone added)

The microstructural analysis of composites with the addition of fiberglass aimed to observe the matrix-fiber interaction, such as its bonding and its possible alkaline attack on the fiberglass.

Figure 12a and 12b show the presence of fiber clusters in the M_{10} cementitious matrix, evidencing the formation of voids around the interface between the fibers and the matrix, possibly caused by the tension applied during the process, resulting in a slight disintegration of the MOS matrix. In this case, was verified the breakage of the fiber (indicated by circle in the figure), suggesting that the tension transfer between the fiber and the matrix was effective, indicating that there was no loss of adhesion between

fiber and matrix. **Leaf-shaped crystals** of Magnesium Hydroxide are also observed in the fiberglass filaments. However, there are no hydration products adhered directly to the fibers, only near them, and it is possible to notice the integrity of their surface without signs of corrosion. EDS showed the predominance of Magnesium, Oxygen and Silicon, with the presence of Zirconium (see Fig. 12b), which is used in the composition of AR fiberglass. Figure 12c illustrates the SEM image of the M_{20} sample with fiber addition, demonstrating an adhesion between the fiber and the matrix similar as observed in M10. However, an increase in deposited material on the surface of the fiberglass was noted. Despite the increase in voids, the good adhesion between the fiber and the matrix was reflected in greater Flexural Strength in both composites, proving the transfer of stresses without slipping when the material is subjected to load. In addition, an increase in matrix porosity was identified with the presence of spherical pores, as shown in Figure 12d. Despite the presence of spherical pores, the fibers remained adhered to the matrix, indicating good interaction fiber-matrix. The fact that M_{20} presented a slightly lower resistance than M_{10} may be related to the higher void index, and the difference in resistance between the two composites is quite small. This similarity in the results is also reflected in the Physical Properties tests, which indicated similar behaviors between the M_{10} and M_{20} composites.

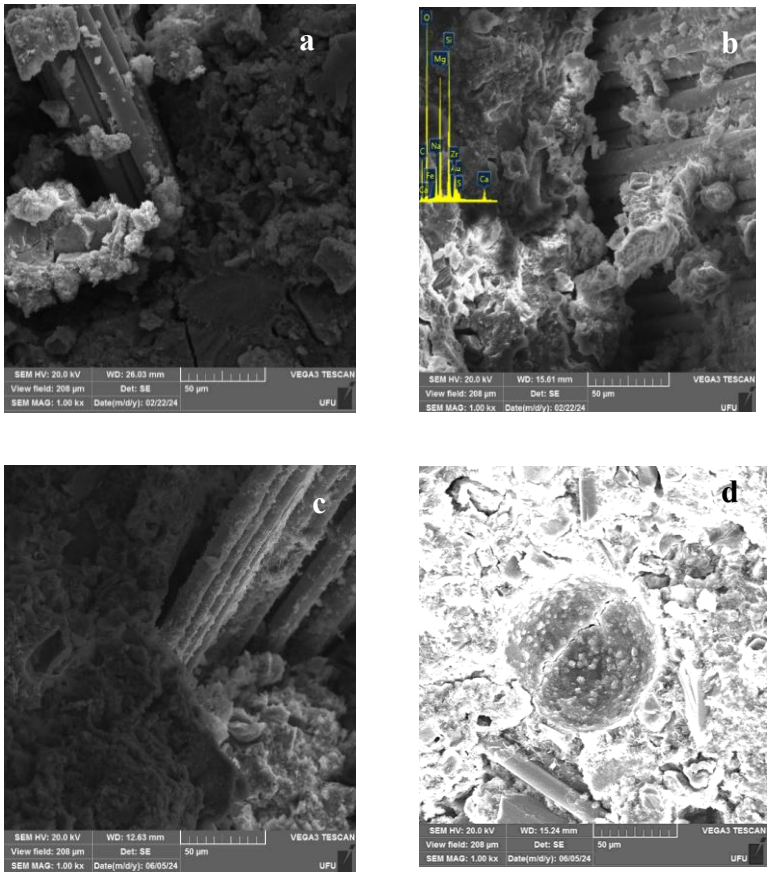

Figure 12. SEM imagens from MOS composites with fiberglass added. a) and b) M_{10} c) and d) M_{20}

IV. CONCLUSION

The results obtained allowed us to conclude that the substitution of part of MgO by limestone in was beneficial for the Dimensional Stabilization of the composite, reducing its propensity to cracking of the MOS. With substitution levels between 10% and 20%, the pores acted to relieve internal tensions generated by the expansion of MgO, resulting in an improvement in Flexural Strength. The addition of fiberglass showed to be effective in controlling shrinkage, reducing the cracks' formation and increasing tensile and Flexural Strength. High levels of limestone compromised the mechanical properties of the composite, perhaps due to the reduction of the Molar Ratio and the inert behavior of the limestone. The retarding effect of limestone also appeared to limit the formation of the appropriate Subsulfated Phases,

impairing the development of 3-Phase and 5-Phase. In addition, the increase in porosity promoted by limestone, generated a greater amount of water available that did not participate in the hydration of MgO, resulting in lower Density and Compressive Strength. In addition, the control of MOS exudation is essential to preserve the Magnesium Sulfate content, which is important in the formation of Subsulfated Phases, optimizing the mechanical strength of the material.

ACKNOWLEDGEMENTS

The authors thanks IBAR Nordeste, Owens Corning Fiberglass and Decorlit for donating the materials used in this research.

REFERENCES

[1] Winnefeld, F.; Epifania, E.; Montagnaro, F., Gartner, E.M. (2019). Further studies of the hydration of MgO-hydromagnesite blends. Cement and Concrete Research, Volume 126. https://doi.org/10.1016/j.cemconres.2019.105912

[2] Hay, R.; Celik, K. (2022) Enhancing carbonation of magnesium oxide (MgO) cement (RMC)-based composites with calcined limestone. CEMENT, Volume 9. https://doi.org/10.1016/j.cement.2022.100037

[3] Vandeperre, L.; Liska, M.; Al-Tabbaa, A. (2007) Reactive magnesium oxide cements: properties and applications. Sustainable Construction Materials and Technologies, Taylor and Francis, 9781003061021, London.

[4] Wang, R.; Qin, L.; Gao, X. (2020) Mechanical strength and water resistance of magnesium oxysulfate cement based lightweight materials. Cement and Concrete Composites. Volume 109. https://doi.org/10.1016/j.cemconcomp.2020.103554.

[5] Gomes, C.M.; Dionisio, A. S. O. (2018) Chemical phases and microstructural analysis of pastes based on magnesia cement, Construction and Building Materials, Vol. 188, P. 615-620. https://doi.org/10.1016/j.conbuildmat.2018.08.083

[6] Gomes, C. M.; Oliveira, A. S. O. (2020) Effects of filler carbonates on magnesium-oxide based pastes. Construction and Building Materials, Vol. 262. https://doi.org/10.1016/j.conbuildmat.2020.119913.

[7] Li, Q.; Zhang, L.; Gao, X.; Zhang, J. (2020) Effect of pulverized fuel ash, ground granulated blast-furnace slag and CO2 curing on performance of magnesium oxysulfate cement. Construction and Building Materials, Vol 230. https://doi.org/10.1016/j.conbuildmat.2019.116990.

[8] Hu, Z., Guan, Y., Chang, J., Bi, W., & Zhang, T. (2020). Effect of Carbonation on the Water Resistance of Steel Slag—Magnesium Oxysulfate (MOS). Cement Blends. *Materials*, *13* (21). https://doi.org/10.3390/ma13215006

[9] Zeng, X.; Yu, H.; Wu, C. (2019) An Overview of Study on Basic Magnesium Sulfate Cement and Concrete in China (2012–2019), KSCE Journal of Civil Engineering, Vol 23, Issue 10, Pag 4445-4453. https://doi.org/10.1007/s12205-019-0199-7

[10] Hao, Y.; Li, C.; Zhao, F. (2019) Study on water resistance modification of magnesium oxysulfate cement. IOP Conference Series: Materials Science and Engineering, v. 493, n. 1. http://doi.org/10.1088/1757-899X/493/1/012079

[11] Ruan, S.; Unluer, C. (2016) Comparative life cycle assessment of reactive MgO and Portland cement production. Journal of Cleaner Production, Vol. 137, Pag. 258–273. https://doi.org/10.1016/j.jclepro.2016.07.071

[12] Marmal, G.; Savastano H. (2017) Study of the degradation of non-conventional MgO-SiO_2 cement reinforced with lignocellulosic fibers. Cement and Concrete Composites, Vol. 80, Pag. 258–267. https://doi.org/10.1016/j.cemconcomp.2017.03.015

[13] Gomes, C. M. (2013) Alternative binder for fibercement building materials. Advanced Materials Research, Vol. 753, Pag. 616-622. DOI:10.4028/www.scientific.net/AMR.753-755.616

[14] Sales, H. A. (2018) Desempenho mecanico e durabilidade de placas planas a base de oxido de magnesio. Dissertacao de Mestrado. Faculdade de Engenharia Civil, Arquitetura e Urbanismo, Universidade de Campinas.

[15] Associacao Brasileira de Norma Tecnicas - ABNT NBR 13276 - Determination of the Consistency Index (2016)

[16] Associacao Brasileira de Norma Tecnicas - ABNT 9778 - Hardened mortar and concrete - Determination of water absorption, void index and density (2016)

[17] British Standards Institution. BS EN 196-3 - Methods of testing cement. Determination of setting times and soundness (2016)

[18] American Society for Testing and Materials - ASTM C348- Standard Test Method for Flexural Strength of Hydraulic Cement Mortars (2021)

[19] American Society for Testing and Materials - ASTM C349 - Standard Test Method for Compressive Strength of Hydraulic Cement Mortars (using broken prism portions of the flexure tests) (2024)

Authors

Kalita Cristina Araujo, Civil Engineer from Pitagoras College in 2018. She received a 24-month CNPq scholarship as a researcher in a partnership with SEBRAE-MG, working with more than 80 companies using an innovation methodology and developing scientific articles and case studies in the field of entrepreneurship. Master's degree in Civil Engineering by Federal University of Uberlandia (UFU). Her research interests include the study of magnesium oxysulphate compositions, as well as the study of fiberglassin MOS cement paste.

Antonio de Paulo Peruzzi, Civil Engineer from University Federal of Sao Carlos (UFScar) in 1997, Master in Architecture and Urbanism from the University of Sao Paulo (USP) and Ph.D in Architecture, Urbanism and Technology from the University of Sao Paulo (USP). P.D, in Science and Material Engineering (USP) in light concrete. Works as a professor and researcher at the Faculty of Civil Engineering (FECIV) of the University Federal of Uberlandia (UFU) in fiber-reinforced concrete, non-metallic bars (GFRP) and magnesium oxide-based composites.

Carlos Marmorato Gomes, Civil Engineer from the University of Sao Paulo (USP) in 1995, Bachelor in Business Administration from the Association of Escolas Reunidas in 1993, Master in Architecture and Urbanism from the University of Sao Paulo (USP), Ph.D. in Science and Material Engineering from the Institute of Physics of Sao Carlos (USP). P.D. -I in Construction Materials - FZEA/USP and the P.D. -II in LSF building system - IAU/USP. Works as professor and researcher at the School of Civil Engineering, Architecture and Urbanism at UNICAMP in fiber-reinforced and magnesium oxide-based composites composites. Member of scientific and regulatory committees, also participates as a consultant and service provider to various companies through university extension activities.